Paravani, a puzzling lake in the South Caucasus

Erwan Messager, Jérôme Poulenard, Pierre Sabatier, Anne-Lise Develle, Bruno Wilhelm, Sébastien Nomade, Vincent Scao, Charline Giguet-Covex, Ulrich Von Grafenstein, Fabien Arnaud, et al.

Paravani, a puzzling Lake in the South Caucasus

Erwan Messager (a), Jérôme Poulenard (a), Pierre Sabatier (a), Anne-Lise Develle (a), Bruno Wilhelm (b), Sébastien Nomade (c), Vincent Scao (c), Charline Giguet-Covex (a), Ulrich Von Grafenstein (c), Fabien Arnaud (a), Emmanuel Malet (a), Ana Mgeladze (d), Estelle Herrscher (e), Mathilde Banjan (a) Arnaud Mazuy (f), Jean-Pascal Dumoulin (g), Soumaya Belmecheri (h), David Lordkipanidze (d).

a. EDYTEM, Université Savoie Mont-Blanc, CNRS, Le Bourget du Lac
b. University Grenoble Alpes, LTHE, 38 000 Grenoble
c. LSCE/IPSL, Laboratoire CEA-CNRS-UVSQ et Université de Paris-Saclay Domaine du CNRS, Bât. 12, Avenue de la Terrasse, 91198 Gif sur Yvette, France
d. Georgian National Museum. 3, Rustaveli Avenue, 0105 Tbilisi.
e. Aix Marseille Univ, CNRS, Minist Culture, LAMPEA, Aix-en-Provence, France
f. UMR 7264, CEPAM-CNRS Nice Université. Campus SJA3, 06357 Nice Cedex 4
g. UMS 2572, Laboratoire de Mesure du Carbone 14. CEA Saclay, 91191 Gif sur Yvette
h. Laboratory of Tree-Ring Research, 1215 East Lowell Street, Tucson, AZ 85721

Abstract

Sediments of Lake Paravani, the largest natural lake in the South Caucasus, were analysed to reconstruct the millennial history of the environment. Pollen analysis, previously undertaken on the first core retrieved in the middle of the lake, revealed a vegetation history for the last 12 millennia. As part of the present study, a new core was taken from the north-western part of the lake. Pollen analysis was performed on this new core with the same methodology as for the previous one. A sedimentological and geochemical analysis was also conducted on both cores in order to gain an understanding of the dynamics of erosion in the catchment area in response to landscape modifications. The results show that the sediment deposits within Lake Paravani yield rather complex and puzzle-like palaeoecological records. Despite the differences between the two records, correlations have been made that are supported by the 14C dates. By combining all of the data from both cores, it was finally possible to reconstruct the puzzle of the environmental history recounted by the Lake Paravani sediments. This reconstructed history is composed of four main phases: 1. a steppic environment marked by pronounced erosion processes from 12 000 to 10 000 cal. BP; 2. a transition phase characterized by the expansion of grasses (Poaceae) from 10 000 to 9-8 000 cal. BP; 3. a more forested phase from 9-8 000 to 2 000 cal. BP, during which the erosion fluxes decreased; and 4. a decline in tree cover probably due to human activities over the last 2 millennia.

Introduction

The South Caucasus is located at the crossroads of Europe, the Middle East and Central Asia (Fig. S1) and provides an original archaeological chronicle, influenced both by its proximity to the Levant (the cradle of agriculture in Europe), and its specificity as a mountainous region. Therefore, the question of the environmental trajectories in the South Caucasus is crucial for understanding the regional demography and the socio-economic dynamics of past societies. Well-dated palaeoecological records are scarce and the vegetation history is not yet fully-understood. A research effort has been conducted in this region over the last ten years to reconstruct the history of palaeoenvironments, and in particular the vegetation (Connor and Sagona, 2007; Ammann, 2009; de Klerk et al., 2009; Connor, 2011; Messager et al., 2013, 2017; Joannin et al., 2014; Leroyer et al., 2016; Connor et al., 2018). Sites favourable to sediment archiving, such as lakes, are particularly targeted. Lake Paravani, located on the Javakheti Plateau, is the largest lake in Georgia and was the subject of an early study (Messager et al., 2013). In this previous work, the vegetation history was reconstructed based on one core sampled in the middle of the lake. This method, based on one core, is common practice in palaeoecological studies using lake sediment (Cohen, 2006). Based on this study, a three-phase vegetation history emerged for the Javakheti Plateau: 1. a steppic environment under a cold and arid climate from 12 000 to 8 500 cal. BP, 2. a more forested environment from 9-8 000 to 2000 cal. BP and 3. a decline in tree cover during the last 2 millennia due to human impact.

Other pollen analyses carried out in similar contexts (volcanic plateaux in the Lesser Caucasus, elevation close to 2000m) also revealed a major palaeoecological change (transition from steppe to more forested and/or increasing hygrophilous vegetation) which occurred at 9-8 000 cal. years BP (Joannin et al., 2014; Leroyer et al., 2016; Messager et al., 2017). In South-western Georgia, a region close to the Black Sea, which represents a major source of moisture, the vegetation history seems to differ somewhat, with forest expansion occurring earlier, around 10 000 cal. BP at an elevation of 2000 m asl (Margalitadze, 1995; Connor et al., 2018).

Over recent years, we have collected several other cores from Lake Paravani with two objectives: 1. to better understand the sediment processes in this large, shallow lake and 2. to find sediments dating to the Early Holocene that might help us to clarify the question of forest expansion in that region (chronology, climatic control, etc.). Most of the retrieved sequences are fragmentary (with many hiatuses) or are very short (Fig. S2). In this paper, we propose to analyse and compare the two longest and most complete sequences from Paravani. A multiproxy approach combining sedimentology and mineral geochemistry was adopted to gain a better understanding of the relationships between the lake sediment records and the erosive processes that have affected the watershed. New pollen analysis was undertaken on core PAR12-04 and the results were compared to

pollen data from the previously published core PAR09-01. Finally, based on the sediment and pollen data, we have been able to reconstruct the chronology and the patterns of the Paravani deposits. The overall goal of this study is to improve scientific knowledge of the climate and vegetation histories of the highlands, and to understand their relationships with the erosive processes and the functioning of the lake over the last 12 millennia.

Regional and local setting

Lake Paravani is located on the Samtskhe-Javakheti Plateau, at 2073m a.s.l., between two main volcanic domains (Fig. 1). The eastern part is dominated by old (3-1 Ma) basaltic lavas and andesitic basalts (Nomade et al., 2016), composed of less differentiated and under-saturated Ti rich rocks (Javahketi plateau, *sensu strico*). The western part is mainly composed of differentiated rocks such as dacites and andesites. These rocks all belong to the most recent activity (last 500 ka) of the Samsari Ridge (Lebedev et al., 2008, Nomade et al., 2016). This volcanic ridge (Fig. 1) corresponds to 20 principal volcanic domes. The watershed (234 km^2) of Lake Paravani (surface of 37.5 km^2) straddles the two main volcanic units.

The Javakheti region possesses the largest number of lakes and marshes within the Caucasus (Matcharashvili et al., 2004). Inherited glacial morphologies and formations are widespread on the Javakheti Plateau, but no active glacier currently exists. The climate of the Javakheti Plateau is continental with long, cold winters and short, cool summers. The mean annual temperature is ca. 5.3°C and the annual precipitation rate is ca. 500-600 mm with a maximum in late spring and early summer, and a minimum in January (Matcharashvili et al., 2004). The most widely distributed vegetation community is mountain steppe, dominated by grasses (Poaceae family, e.g. *Festuca* spp. or *Stipa* spp., Fig. 2). Forest communities are mostly absent from the plateau and only two small areas of sub-alpine forest still exist, one on the eastern part of Lake Kartsakhi and a second on the side of Mt Tavkvetili (Fig. 2) (Arabuli et al., 2008). While the plateau is steppic, different types of forest exist nowadays on the northern ranges (Bohn et al., 2000).

Material and methods

1. Coring sites

In this study, we investigate two cores collected in lake Paravani (Fig. 1): core PAR09-01 retrieved in 2009 from the middle of the lake at a water depth of 3 m (Messager et al., 2013) and a new core PAR12-04 retrieved from the littoral area at a water depth of 2.8 m (41.465°N, 43.799°E) in 2012.

105 **2. XRF core scanner**

106 The relative major element contents were measured every 0.5 cm on PAR09-01 and PAR12-04 using
107 a XRF Avaatech core scanner (EDYTEM laboratory, Université de Savoie Mont-Blanc). An X-Ray beam
108 was generated with a rhodium anode and a 125 µm beryllium window which allows a voltage range
109 of 7 to 50 kV and a current range 0 to 2 mA. The analytical settings were adjusted at 10 kV and 1.5mA
110 in order to detect light elements (Al -> Fe). Each individual power spectrum was transformed by the
111 deconvolution process into relative contents (intensities) expressed in counts per seconds (cps).
112 Principal component analysis was applied to XRF data in order to decipher sedimentary processes
113 controlling the lake sedimentation using R statistical software and the multivariate analysis package
114 FactomineR (Fox, 2016; Lê et al., 2008; R Core Team, 2018).
115
116 **3. Magnetic Susceptibility**

117 For magnetic susceptibility (MS) analyses, two different protocols were used. The core 09-01 was
118 sampled using $2cm^3$ sampling plastic cubes at 2 cm resolution. The core PAR12-04 was sampled using
119 a U-channel. The U-channel was then directly measured with a 1 cm resolution. MS was measured at
120 the Laboratoire des Sciences du Climat et de l'Environnement (LSCE) at Gif-sur-Yvette (France) using
121 a Bartington© MS3 model, and the MS values obtained were normalized to sample weights (wet).
122
123 **4. Loss On Ignition analysis**

124 Loss On Ignition (LOI) analyses were carried out to estimate the organic content of the sediment,
125 following the procedure used by Heiri et al. (2001). Forty samples, collected at 1 to 3 cm intervals,
126 were dried. Since organic matter is oxidized to carbon oxide, dioxide and ash at temperatures
127 between ca. 200 and 500ºC, the record of sample weights before and after heating (ignition at 550°C
128 during 5h) allows us to estimate the weight of the organic content. The heating of several test
129 samples to 950°C (for a period of 2h) in order to estimate the carbonate content yielded so negligible
130 a weight loss (<1%) that this step of the process was abandoned.
131
132 **5. Chronology**

133 The core chronology for PAR09-01 and PAR12-04 is based on 10 and 16 AMS ^{14}C dates respectively,
134 determined on bulk sediment (Table 1).
135
136 Clam v2 (Blaauw, 2010), written for the open-source statistical software 'R', was used to calibrate the
137 ^{14}C ages with the Intcal13 calibration curve (Reimer et al., 2013) and to construct an age-depth model
138 for cores PAR09-01 and PAR12-04. An age-depth model, already published for core PAR09-01 core

(Messager et al., 2013), has been refined using Clam v2 software, based on the IntCal13 calibration curve (Reimer et al., 2013).

6. Pollen analysis

Thirty-three samples were taken at 1 to 5 cm intervals for pollen analyses. For each sample, 1-2 g of sediment were processed following standard methods in palynology, using HCl, KOH baths (Faegri and Iversen, 1989) and heavy liquid (d:2) flotation (Girard and Renault-Miskovsky, 1969; Goeury and Beaulieu, 1979). If significant amounts of silica particles remained, a HF bath was used. After treatment, the residue was suspended in glycerol, mounted onto microscope slides and counted using "Zeiss standard™“ and "Leica DM 1000" microscopes. Pollen grains were identified using atlases of European and Mediterranean pollen types (Reille, 1992; Beug, 2004). The pollen concentration ranges from 10 to 30,000 grains. g^{-1} in the A12 unit, from 30 to 60, 000 for the B12 unit, and from 60 to 250, 000 for the C12, D12 and E12 units. The total pollen sum ranges from 300 to 349 in most samples, except five samples in which pollen grains were less abundant: i.e. samples 72, 86, 92, 96, and 99 (from 205 to 270 pollen grains counted). Percentage calculations were based on the total terrestrial pollen (AP: Arboreal Pollen + NAP/Non Arboreal Pollen), excluding Cyperaceae, and moss and Pteridophyte spores.

Results and Interpretation

1. Sediment analysis

Lithology and sediment description

The stratigraphy of PAR12-04 is divided into five different units (A12 to E12) from the base to the top of the sequence (Table 2, Fig. 3). Initially the unit boundaries were visually identified, and then they were compared to the tipping point identified within the xrf data.

Sediment samples were collected in each unit to prepare smear slides. An illustrative picture of bulk sediment for each unit is presented along the stratigraphy in the supplementary Fig. 3. The observations of the slides provide an estimation of diatom abundance in each unit. All units contain a significant quantity of diatoms, except unit A12, which is diatom-free. The richest units are B12 and D12. The lithology of core PAR09-01 (Fig. 3) has already been described by Messager et al. (2013). The three initial units A, B, C have been renamed A9, B9 and C9 for this paper (Table 2). Following the same methodology used for PAR 12 04, the boundary between units B9 and C9 has been moved by 2.5 cm (29 cm instead of 31.5 cm) based on the shift recorded at 29 cm by XRF data.

LOI analysis

The LOI tests at 950°C did not reveal significant carbonate content in the Paravani sediment. The LOI at 550°C is presented in figure 3. For core PAR 12-04, the LOI is lower than 10% for the lowest units A12 and B12. The LOI values fluctuate from 12 to 16% for C12, from 10 to 12% for D12 and from 10 to 18% for E12. For core PAR 09-01, units A9 and B9 present low contents of organic matter. The highest LOI values (up to 12%) are recorded in the upper unit, C9.

Magnetic susceptibility

For core PAR12-04, the magnetic susceptibility displays high values for units A12 and B12, lower values for C12 and D12, and a progressive increase within unit E12 (Fig. 3). The magnetic susceptibility curve for PAR09-01 has already been described elsewhere (Messager et al., 2013).

XRF analysis

Down core variations

Al, Si, K, Ca, Ti and Fe XRF intensities are presented in figure 3 for both cores. In PAR09-01, all elements reach their highest values in A9 (Fig. 3). In B9 and C9, they decrease gradually up to the top of the sequence. In PAR12-04, the highest values for all XRF indicators are observed in A12 and B12. Detrital inputs then decrease gradually from C12 up until the upper 10 cm of E12, where they

192 decrease again sharply. Surprisingly, this decrease occurs for all elements and seems to be due to a
193 water content effect. All elements roughly follow the same trend in both cores, except for small
194 variations that are particularly perceptible in the calcium XRF signal.

195 *Principal component analysis*

196 Principal component analysis (PCA) was applied to the XRF results in order to decipher sedimentary
197 processes controlling the geochemistry of cores PAR09-01 and PAR12-04 (Fig. 4). PCA was performed
198 on major elements (Al, Si, K, Ti, Ca and Fe intensities). In both cores, nearly 80% of the total variance
199 is supported by high loadings of all elements on dimension 1 (Dim1). This could be due to a strong
200 imprint of detrital inputs and the absence of other XRF indicators, which could be associated with
201 other processes (organic production and/or redox variations). However, variable projections for both
202 cores indicate a similar trend between two end-members in the detrital inputs, which could be
203 associated with a balance of fine to coarse particles (e.g. Fe and K against Ca and Si), and/or
204 geochemical changes due to changes in source of sediments (Sabatier et al., 2010; Wilhelm et al.,
205 2016a).
206

207 Individual projections are sorted by units (Fig. 4). In PAR09-01, unit A9 is strongly supported by Dim1,
208 which indicates that detrital processes dominate the signal in this unit (mainly K, Al, Fe
209 contributions). Conversely, in unit B9 and then in C9, we observe a gradual shift toward a negative
210 correlation to Dim1; this indicates that these units are characterised by less detrital inputs and other
211 controlling processes. In PAR12-04, the trajectory scheme of the unit is roughly the same as for
212 PAR09-01, with a strong correlation of A12 individuals to Dim1 and then a gradual shift to negative
213 loadings from B12 to E12.

214 *Geochemical relationships\ratios*

215 Based on the XRF data, three ratios have been calculated: Si/Al (Fig. S3), Fe/Al and Ti/Al (Fig. S4).
216 - The Si/Al ratio can be considered as a tracer of biogenic silica (Köning et al., 2002, Ragueneau et al.,
217 2005). In PAR09-01, the Si/Al ratio is low in A9, and increases sharply at the transition between A9
218 and B9. It remains stable in B9 and C9, except in the 40-20 cm interval where higher values are
219 observed. In PAR12-04, the Si/Al ratio is low in A12 and increases slightly in B12. It exhibits
220 fluctuations between high values in B12 and D12 and lower values in A12, C12 and E12. Finally, a
221 gradual increase is observed in the upper 10cm interval of the core.
222 In the Paravani sequence, the SI/Al ratio covariates with diatom abundance (Fig. S3) and closely
223 matches the other indicators of climate improvement (pollen, OM, etc.). We could interpret it as a

first marker of biogenic silica, but it should be used with caution because the Si contribution of the bedrock can also modify the Si/Al.

- The Ti/Al and Fe/Al ratios have been tested in order to decipher the different sources of the mineral input (See Fig. S4). Different volcanic formations, such as basalt-basaltic andesite and dacite-andesite, occur in the Paravani watershed (Fig. 1). Because the basalt-basaltic andesite is rich in Ti and Fe (Nomade et al., 2016), the rise in Ti/Al and Fe/Al ratios could be interpreted as indicating a greater contribution from these formations in the detrital input. Both ratios exhibit the same trend (Fig. S4). In PAR09-01, the values are low in A9, increase slightly in B9 and increase simultaneously in C9. In PAR12-04, Fe/Al and Ti/Al ratios are relatively stable and remain low all along the sequence, except towards the top of the sequence, where they both increase sharply. They yield an ambiguous signal that is probably influenced by the double origin of the silica (bedrock and biogenic silica). Thus, the core scanner XRF data do not permit us to carry out source analysis satisfactorily. It is for this reason that the specific task of quantifying detrital and biogenic inputs will be undertaken using WD-XRF.

Overall, in the case of this study of the Paravani sediments, the XRF core scanner is used to some extent as a correlation tool and as a preliminary indicator of biogenic silica contribution.

Chronology

Sixteen radiocarbon measurements were performed on organic matter from bulk sediment collected in core PAR12-04 (Table 1). Among the 16 samples analysed, one date was rejected from the age-depth model (Fig. 5); the Poz58699 sample at 93.5 cm (Table 1), dated to 11240 BP, is clearly too old, probably due to the presence of reworked material.

A number of hiatuses have been identified based on the combination of radiocarbon ages and abrupt changes in geochemistry (XRF data). Two main hiatuses were identified at depths of 84.5 cm (between B12 and C12) and 69 cm (between C12 and D12). Deposition of the C12 unit began around 5 100 and stopped at 4 650 cal. year BP. A hiatus of 1 850 years precedes the onset of the deposition of D12 at around 2800 cal. years BP. The other hiatus, which occurs between units B12 and C12, lasts more than 4 000 years.

For core PAR09-01, ten samples were radiocarbon dated (Messager et al., 2013). Based on pollen and XRF data, the B12 phase recorded in PAR12-04, ranging from 10 500 to 9 300 cal. years BP, is not recorded in the PAR09-01. As a result, a hiatus has been proposed at a depth of 69 cm (Fig. 5). The underlying sediments are older (two radiocarbon dates earlier than 12 000 cal. years BP) and the continuous record begins at 69cm, or at 8250 cal. years BP (Fig. 5).

2. Pollen results

Results of the pollen analyses are presented in the pollen diagram below (Fig. 6). Local Pollen Assemblage Zones (LPAZ) have been defined (Birks and Birks, 1980) using the CONISS method (Grimm, 1987). Five main LPAZs have been identified in the PAR12-04 pollen record (Fig. 6):

- LPAZ1 (depth: 105.5-91 cm): The first zone is characterized by the prevalence of herbaceous pollen taxa. Amaranthaceae-Chenopodiaceae (42.9-56.8%) and *Artemisia* (12.7-24.3%) dominate the pollen assemblages. Open vegetation is also attested by the abundance of other herb taxa, such as Poaceae, Asteraceae (Asteroideae, Cichorioideae), Caryophyllaceae. The Alimsataceae family is well represented (1.5-7%). The xeric and steppic taxon, *Ephedra distachya* t., is present in every sample of this zone (0.5-2.4%). In this LPAZ, just a few tree pollen grains of *Betula* (0.4-1%), *Quercus* (0.5-1.5%), *Fagus* (0-0.8%), *Pinus* (0-1.5%) and *Corylus* (0-0.5%) have been identified.
- LPAZ2 (depth 91-85 cm): This zone is marked by an abrupt decrease of Amaranthaceae-Chenopodiaceae (17.6-26.2%), while Poaceae values rise significantly, from 18.5% to over 33%. There is a slighter decrease in *Artemisia* while the other herbs present rather stable pollen values. This zone records the last significant occurrence of the Alimsataceae family. The AP values increase (from 14.7 to 28.9%) in LPAZ 2 due to the progressive expansion of deciduous trees such as *Quercus*, *Fagus*, *Betula* and *Carpinus*. Nonetheless, *Ephedra distachya* is still well represented, attesting to the steppic character of the vegetation.
- LPAZ3 (depth 85-68 cm): This zone is characterized by low values of herbaceous pollen (NAP ranges from 35.8 to 50.6%) and high pollen values for tree pollen taxa, such as *Pinus* (19.3-35.2%)*, Betula* (1.9-3.4%)*, Carpinus* (2.3-7.1%)*, Fagus* (3.8-6.9%)*, and Quercus* (10-15%). *Ephedra distachya* is not recorded.
- LPAZ4 (depth 68-58cm): This zone is marked by the lowest herbaceous pollen values of the record (NAP ranges from 21 to 26.6%) due to low Poaceae, Amaranthaceae-Chenopodiaceae and *Artemisia* pollen values. LPAZ4 is also characterised by the highest values of *Pinus* in the sequence (36.8-52%).
- LPAZ5 (depth 58-0cm): In this zone, some of the herbaceous pollen taxa, such as Asteraceae Asteroideae, Ast. Cichorioideae and Poaceae, show increasing frequencies. Pollen indicators of human activities display a continuous curve (Fig. 9). Indeed, the taxa *Plantago*, an indicator of pastoral activity, and Cerealia are both well recorded in this zone. Deciduous trees present stable pollen values, but the *Pinus* values tend to decrease slightly along the LPAZ. *Abies* tends to disappear while *Picea* presents increasing pollen values. This zone documents a more open landscape than LPAZ4.

Discussion

1. Why a puzzling lake?

The sediment analysis of PAR12-04 and PAR09-01 sequences shows that the deposits within Lake Paravani yield rather complicated and puzzle-like palaeoecological records. To reconstruct the history of past environments, palaeoecologists traditionally use the sediments recovered from the deepest and/or central part of the lake (Cohen, 2003). Such a sequence is assumed to be representative of the lake deposits. Since the sequence comes from the lowest bathymetric point (lowest bottom), the occurrence of hiatuses due to very low sedimentation, or none at all, during emerging phases is limited. Even though, core PAR09-01 was taken from the central part of the lake, and at the maximum depth (3m), its sequence presents a hiatus of several thousands of years at a depth of 69 cm (Fig. 5). Indeed, when comparing the pollen data from both cores, the period covered by the B12 unit in PAR12-04 (10 500 to 9 300 cal. years BP), characterized by very high Poaceae values and a slight increase of arboreal taxa, is not recorded in PAR09-01 (Fig. S5). The absence of a hiatus for this time period in core PAR12-04, a core retrieved in a slightly higher bathymetric point (2.8m), is an unexpected result because in theory, this upper point, located closer to the shoreline, is more likely to be affected by emerging phases. The PAR12-04 sequence presents hiatuses of 4 000 and 1 850 years at depths of 84.5 and 69 cm, respectively. Consequently, both cores yield two different records with asynchronous hiatuses. Correlating the different units turned out to be a real challenge. The curves provided by XRF core logging (which is an efficient tool for correlating lake sequences) were not easy to disentangle (Fig. 3). Their comparison is rendered particularly complex by the hiatuses and variable concentrations of diatoms (Fig. S3). Indeed, the increasing diatom concentration dilutes the detrital input and may have a significant effect on the XRF results (dilution of other elements by biogenic silica). If the diatom bloom is localized in the lake, some cores might record diatoms while others would not. Dissimilar sediment sequences within a single lake have already been observed in several lakes (Anderson, 1986; Beaudoin and Reasoner, 1992). However, in previous works, the cores came from different depths (contrasted bathymetry). In the case of Lake Paravani, the lake bottom is almost flat and there is no delta which might generate significant differences in sediment facies. The presence of hiatuses at Paravani could be explained by the low water depth (facilitating bottom emergence during low lake levels), but how do we explain the absence of synchronicity for these hiatuses? One hypothesis that might be forwarded is the effect of earthquakes. In fact, lacustrine sedimentation can be highly sensitive to regional earthquake activity with slope failures, violent waves and seiche effects causing hiatuses (Chapron et al., 2016, Wilhelm et al., 2016). In the Samskhe-Javakheti, which is known as a seismically active region (Kachakhidze et al., 2003), past earthquakes could have modified the lake sedimentation. Numerous prehistoric and historical earthquakes have already been documented in the region (Philip et al., 2001; Ritz et al., 2016). No

traces of homogenite or turbidite have been observed in the sequences. Moreover, in such a large and shallow water body, it is difficult to imagine that the observed hiatuses could be the result of mass wasting deposits (displaced blocks of sediment), an earthquake-triggered mechanism that has been clearly identified in the Alps (Wilhelm et al., 2016). The Paravani Lake seems to be on a major fault (Nomade et al., 2016), within a highly seismically active area, where earthquakes of a 6-7 magnitude and surface ruptures are historically attested (Ritz et al., 2016). Without detailed bathymetry mapping, however, we cannot discuss the potential of underwater fault activity leading to sediment hiatuses in the upper compartments (Beck et al., 2012). Another factor that could have played a role in the sedimentation process is the wind. In shallow lakes, such as Paravani, the wind can directly drive the sedimentation process and hydrodynamics, generating deep erosional surfaces (Nutz et al., 2016). This question deserves further exploration because Paravani is particularly subject to thermal winds during the summer.

Despite the differences between the two records, it is possible to draw correlations (Fig. 7 and 8) based on pollen data and the PCA performed on the XRF data (Fig. 4). These correlations are supported by the ^{14}C dates, thus allowing us to better constrain the chronology of each unit. By combining all of the data from both cores, it is finally possible to reconstruct the puzzle of the environmental history recounted by the lake Paravani sediments (Fig. 7).

2. The environmental history provided by the combination of 09-01 and 12-04 records

Before 10 500 years cal. BP

The A12 and A9 units are mainly composed of detrital sediment (Fig. S3), characterized by high Si, Ca, Ti and Fe inputs (Fig. 3) that reflect erosion processes in the Paravani watershed. The low OM value probably indicates low biogenic production in the lake. Diatoms are almost absent in this deposit (low Si/Al and Fig. S3). At that time, the reconstructed vegetation is composed of steppes and semi-desert steppes. All proxies indicate cold, arid climatic conditions. Regional records dating back further than 10-11 000 years cal. BP are characterised by similar environmental and climatic conditions (Wick et al., 2003; Litt et al., 2009; Van Zeist and Bottema, 1977). Such vegetation, dominated by Amaranthaceae-Chenopodiaceae, is characteristic of glacial phases recorded in the two long regional sequences sampled in Lakes Urmia (Djamali et al., 2008) and Van (Wick et al., 2003; Litt et al., 2014). In the volcanic region of the Armenian-Javakheti plateau (Fig. S1), very limited tree cover has been clearly demonstrated by both the Zarishat (Joannin et al., 2014) and Nariani pollen records (Messager et al., 2017).

From 10 500 to 9 300 cal. years BP

The phase recorded by unit B12 is probably the most interesting part of the PAR12-04 sequence. The deposit is securely dated by three radiocarbon dates and fits well within the Early Holocene period, 10 500 to 9 300 cal. years BP (Fig. 7). This record was not recovered by the first sequence (PAR09-01) sampled in Lake Paravani. The sediment of unit B12 is still characterized by detrital input due to erosion. The sediment displays a very low content of organic matter. Nevertheless, the Si/Al curve indicates an increase in biogenic silica, which is confirmed by the abundance of diatoms in smear slides (Fig. S3). This means that the lake system was experiencing a change, with increasing bio-production. Yet, at the same time, the quantity of organic matter remains low, meaning that not all compartments of the lake system are responding at the same time. This change in lake production may have various causes (e.g. rise in temperature, rise in lake level, etc.).

The pollen assemblages from this phase are marked by a very slight increase of tree pollen values due to a small rise in deciduous trees (Fig. 8). This slight rise in taxa living at lower elevations (*Quercus*, *Carpinus*, *Corylus*, etc.) reflects an initial and slight tree expansion in lower vegetation belts, perhaps even from the western part of the South Caucasus (by long-distance pollen transport). This record fits well with the synchronic expansion of deciduous trees recorded at 10 000 cal. BP (See Fig. S6) in the Didachara sequence in south-western Georgia (Connor et al., 2017). Apart from this regional pollen echo from western areas, the pollen assemblages from this phase are still dominated by herbs (71-85-%). In Western Europe, the post-glacial expansion of temperate trees (Huntley and Birks, 1983; Wick, 2000) was underway by this time, but in the South Caucasus, several records indicate that the environment remained steppic in the early Holocene (Margalitadze, 1995; Messager et al., 2013; 2017; Joannin et al., 2014; Leroyer et al., 2016). This pattern is also observed in other regions of South-Eastern Europe and the Near East (Van Zeist and Bottema, 1977, Bottema, 1986; Stefanova and Ammann, 2003; Wright et al., 2003; Djamali et al., 2008; Djamali et al., 2010; Connor et al. 2013; Leroy et al., 2013, 2014; Ryabogina et al., 2019). Different hypotheses have been proposed to explain the delay in forest expansion: (1) the time lag in tree migration from glacial tree refugia (Leroy et Arpe, 2007); (2) the impact of burning (Roberts, 2002; Turner et al., 2010); (3) a relatively dry early Holocene climate (Stefanova and Ammann, 2003; Atanassova, 2005; Shumilovskikh et al., 2012; Van Zeist and Bottema, 1991; Roberts and Wright, 1993; Stevens et al., 2001, 2006; Wright et al., 2003; Djamali et al., 2010); and (4) a negative feedback from the “Black Lake”, preceding the filling of the Black Sea by Mediterranean waters (Leroy et al., 2013). All of these hypotheses have been addressed and discussed in the context of the neighbouring Nariani pollen record (Javakheti Plateau) (Messager et al., 2017).

For this time period, pollen assemblages from the Paravani B12 unit indicate a major change in the herb communities with a significant decrease of Amaranthaceae-Chenopodiaceae (Fig. 7), which was the dominant taxon recorded at Paravani since 12 500 years cal. BP. This decline of Amaranthaceae-

Chenopodiaceae corresponds to the expansion of Poaceae (Fig. 7). A similar vegetation dynamic was observed at Nariani between 10 200 and 9000 cal. years BP (Messager et al., 2017). Such a pattern (i.e. decline of semi-desert, expansion of grassland and very slight rise in tree cover) is also described from the Lake Van sequence (Fig. S6) between 11 500 and 9000 cal. years BP (Wick et al., 2003; Litt et al., 2009). This new pollen data from Paravani, dating back to the early Holocene, confirms the vegetation history reconstructed in Nariani (Fig. 2, Fig. S6). Based on this change in the herb community, a first climatic hypothesis was proposed (Messager et al., 2017), namely that this period is characterized by an increase in annual precipitation. Geochemical and isotopic indicators from Lake Van (Lemcke and Sturm, 1997; Wick et al., 2003), Lake Eski Acigöl (Roberts et al., 2001; Jones et al., 2007) and Nar Gölü (Dean et al., 2015) in Turkey (Fig. S1) show higher water levels and/or lower salinities during the early Holocene. Based on these different indicators, significant annual rainfalls were inferred for the early Holocene. While this climatic trend is regionally recognized, the first Holocene coastal lake terraces on the shores of Lake Van have been dated to 9.5-6 ka (Kuzucuoğlu et al., 2010; Çağatay et al., 2014), slightly younger than the other records. In Armenia, the first sign of increasing rainfall is recorded a bit later (Joannin et al., 2014, Leroyer et al., 2016), around 8000 cal. BP (Fig. S6). At a regional scale, the question of the early Holocene climate and its seasonality is still unresolved. According to the Nariani and new Paravani pollen data, the growing season appears to have remained dry (low precipitation during the spring, limiting tree expansion), while annual rainfall increased. The change in the lake system recorded at Paravani (rising concentrations of diatoms) could be interpreted as a sign of a higher lake level reflecting higher annual precipitation, but the vegetation composition indicates that spring rainfalls remained low.

From 8355 to 1600 cal. years BP

This phase is only fully recorded by unit B9 in PAR09-01, while it is partly represented by units C12 and D12 in PAR12-04 (Fig. 8). The long phase recorded by the B9 unit is clearly marked by a drastic change in sediment composition. As indicated by lower Ti and Fe values in XRF curves, the detrital input decreased during this phase. The decline of erosion might be explained by the development of soils in the watershed and the increasing vegetation cover (see below). The very high Si/Al values could reflect higher biogenic silica production. During this period, both organic matter and biogenic silica reveal higher lake production related to the climatic amelioration, which is, in turn, attested to by the pollen record. Indeed, pollen assemblages reflect relatively forested vegetation growing under warmer and wetter climate conditions. The period ranging from 8000 to 5500 cal. BP is recognized as the period of maximum tree extension in the South Caucasus (Kvavadze and Connor, 2005; Connor and Kvavadze, 2008). In the Paravani record, the pollen data does not reveal a significant human impact from 8355 to 3000-2500 cal. BP (Fig. 8). This observation is rather unexpected because

numerous archaeological sites dating from the Neolithic to the Bronze Age have been identified on the Javakheti Plateau in recent decades. While the Neolithic and Chalcolithic sites mainly occurred in lowlands (Lyonnet et al., 2016; Hamon et al., 2016; Kadowaki et al., 2015), some sites have been discovered on the volcanic plateaus. A rockshelter called Bavra-Ablari, located in the Paravanistkali Canyon, has been excavated in the last few years. The archaeozoological and botanical analyses carried out at Bavra-Ablari demonstrate that the Neolithic (layers dated to 6000-5350 BCE.) and Chalcolithic populations (layers dated to 5000–3900 BCE.) occupying the rockshelter were clearly engaged in a pastoral economy (Varoutsikos et al., 2017). Yet, the pollen spectra from the B9 unit at Paravani does not reveal any signs that grazing impacted on the vegetation at that time (from 8000 to 5500 cal. BP). Moreover, significant impact of livestock on the vegetation has not been detected in other regional pollen records. The main human impact recorded for this period is the extensive use of fire during the Late Chalcolithic (Connor and Sagona, 2007; Connor 2011; Joannin et al. 2014). For the Bronze Age period, several major sites have been excavated in the Samskhe-Javakheti region. The plateau has yielded numerous sites from the Kura-Araxes culture (Early Bronze Age) and from the Middle Bronze Age. The results of investigations carried out on Early Bronze Age sites (Kura-Araxes) point to the development of “high mountain agriculture” marked by the importance of cereal growing (Kvavadze and Kakhiani, 2010; Kakhiani et al., 2015, Messager et al., 2015). The agro-pastoral activities of these populations might have affected the Samskhe-Javakheti environment. However, the Paravani pollen does not record any significant sign of cereal growing or of forest clearance at that time. There may be various reasons for this discrepancy. Pollen records from large lakes such as Paravani mostly reflect changes on a regional scale. This is why pollen assemblages are significantly marked by forests while the signal of human impact is slight. Even if Kura-Araxes sites, dedicated to an agricultural economy, are “frequent” on the Plateau, their environmental impacts were probably not very large in scale and the signal of the environmental perturbations would have been diluted in the regional pollen rain. The location of the sites in the watershed (or not), may also have a major influence on our capacity to detect the intensity of human activities. If we consider the pollen spectra from the C12 unit, the values for pollen indicators of human impact are a little bit higher than in the contemporaneous base of unit B9, and are manifested as a slight increase of *Plantago* and *Cerealia*. The origin of this unit of rapid sedimentation (Fig. 5) is not well understood, but it seems that the deposition process allowed a better record of human impact than the sediment deposited in the middle of the lake (unit B9 from PAR09-01). At the end of unit B9 (and contemporaneous with unit D12), pollen spectra record an increasing human impact and the first noticeable decline in trees (around 2000 cal. years BP).

From 1600 cal. years BP to the present

This last phase is recorded both in PAR12-04 (unit E12) and PAR09-01 (unit C9). It was deposited between 1600-1500 cal. years BP and the present time (Fig. 7). These units are composed of an organic rich sediment, indicating that the lake was still productive (Fig. 8). Diatoms remain well-represented. While organic matter is abundant, the magnetic susceptibility is high in both of these units. For this phase, PAR09-01 and PAR12-04 display different XRF curves for Al, Si, Ti and Fe. These elements decrease throughout unit C9, although the same elements increase in unit E12, up to 10 cm. Thereafter these elements display a decreasing trend for the last 50-100 years (Fig. 3). Therefore, for this phase, it is still difficult to reconstruct the erosion processes based on the XRF core scanner data. According to pollen indicators of human impact (Fig. 8), the last 1500 years are marked by an increasing anthropic imprint. For example, the taxon *Plantago*, a good marker of grazing, presents its highest values in this phase (Fig. 6). Cereal pollen is also well represented. Wheat and barley are mainly self-pollinating plants and their large pollen grains are not well-dispersed by the wind; hence, cereal pollen abundances greatly decrease with distance from cultivated areas. Thus, the *Cerealia* values in the last Paravani phase probably indicate cereal growing within the Paravani watershed (up to 2000m asl). Nowadays, cereals are still grown at this altitude on the Javakheti Plateau; some local varieties of wheat, for example, are cultivated between 800 and 2160m asl (Akhalkatsi, 2016). The decline in tree values initiated during the previous phase continues into the beginning of this phase. The very top of the sequence observed in unit C9 is marked by a scarcity of deciduous trees. It is still difficult to discuss the evolution of the tree cover on the plateau due to the additional pollen rain coming from lower vegetation belts (Kvavadze, 1993; Connor et al., 2004). According to the botanists that have worked on the region (Nakhutsrishvili, 1999; Arabuli et al, 2008), the expansion of the mountain steppes on the Javakheti Plateau is a recent phenomenon, induced by late Holocene deforestation. Certain archival sources, dating back to the 18th century, attest to a forested landscape and thus support this hypothesis (Matcharashvili et al., 2004; Connor, 2011). Based on the pollen analysis, we can presume that the decline of trees on the plateau is a process initiated at least 2300-2000 years ago, but the scarcity of trees is probably a more recent process. However, it remains difficult to pinpoint when this change occurred due to the problem of mixed pollen rains. The question of the origin of the deforestation is also unresolved. According to the pollen evidence, both cereal growing and pastoralism have played a role in shaping the vegetation on the plateau. While grazing is a major driver of the modern vegetation, the intensity of this activity in the past has never been evaluated. Fire setting and mowing may also have played a role in the process of opening up the landscape. In the Aligol and Imera records (both located on the neighbouring Tsalka Plateau, 1500 m asl) an increase in fires is recorded at the beginning of the Classical Era (starting around 2400 cal. BP) and carries on in the subsequent periods (Connor, 2011). The role of fire in the disappearance of fir on this lowest plateau has previously been considered (Connor, 2011).

Additional studies are required in order to chronicle the role of fire in the highlands and to make comparisons with the lower Tsalka plateau. Above all, coprophilous fungi or mammal DNA analyses could be undertaken in order to reconstruct the pastoral history of the Javakheti plateau, and to better decipher its role in the expansion of mountain steppe.

Conclusion

The sediment analysis undertaken on different cores from Lake Paravani reveals the complex history of sediment deposition in the bottom of this puzzling lake. While the sequences are affected by hiatuses, and composed of truncated units, the combination of sediment, organic matter and pollen analysis, with the help of 14C dates, allows us to reconstruct the evolution of the palaeoenvironments in the Paravani watershed over the past 12 000 years. Although the XRF core scanner turned out not to be the most suitable tool to conduct geochemical analysis on the Paravani lake sediment, it has provided the first indications regarding the functioning of the Lake system during the time period in question. The erosion pattern and the lake functioning reconstructed for the Early and Mid-Holocene are in agreement with the vegetation dynamic; both reflect the evolution of the climatic parameters (passage from glacial conditions to post-glacial conditions). The phase of transition between the glacial steppe and the temperate forest is characterised by the expansion of grassland (Poaceae steppe) which replaced the preceding Amaranthaceae-Chenopodiaceae steppe. This phase, not observed in the previous Paravani analysis, was recently identified in the south Caucasus and can be related to a more widely recognized phase of the Early Holocene in the Near East. For the late Holocene (up to 2300 cal. years BP), the pollen record indicates a gradual increase in human impact, but considering the regional (large scale) picture provided by the pollen data, it is still difficult to identify the intensity of the anthropization on the highlands. This period is marked by a change in the sediment delivered to the lake, but the effect of human activities on this erosive pattern is not sufficiently understood. It would be interesting to further investigate the role of the highland populations during the last two millennia in terms of land use and agricultural practices. This would undoubtedly enhance the discussion regarding the processes leading to the deforestation of the Plateau and the subsequent expansion of the mountain steppes which nowadays cover the highlands.

Acknowledgements

This research was partly supported by the "GATES, Georgian Ancient Transcaucasia: Environments and Societies" LIA project, founded by the French Environment and Ecology Institute (InEE, CNRS),

and the ANR-12 JSH3-003-01 Orimil project, directed by E. Herrscher. Thanks to L. Perrin for his significant contribution to the fieldwork logistics. Radiocarbon dates were partly provided by LMC14, Gif-sur-Yvette. We express our gratitude to Rhoda Allanic for correcting the language. We are finally grateful to reviewers for their suggestions that greatly contributed to improve this paper.

References

Akhalkatsi, M., 2016 Ancient Crops Continuing for an Extended Period in Samtskhe-Javakheti Region of Georgia – a Review. Agricultural Research & Technology: Open Access Journal, Volume 3 (1).

Ammann, B., 2009. Reconstruction of vegetation as a tool to understand resources of the past. In: Masserey, C. (Ed.) News of ancient Colchis Arcaeological paleobotanical and historical research program in the Framework of Georgian and Swiss cooperation. Adamantis Press, Caucasian Press, Tbilisi. pp. 5-9.

Anderson, N., 1986. Diatom biostratigraphy and comparative core correlation within a small lake basin Hydrobiologia 143: 105 -112

Arabuli, G., Kvavadze, El., Kikodze, D., Connor, S., Kvavadze, Er., Bagaturia, N., Murvanisze, M., Arabuli, T., 2008. The Krummholz beech woods of Mt. Tavkvetili (Javakheti Plateau, Southern Georgia), a relict ecosystem. Proceedings of the Institute of Zoology 23, 194-213.

Atanassova, J., 2005. Palaeoecological setting of the western Black Sea area during the last 15 000 years. The Holocene 15 (4), 576-584.

Beaudoin, A.B., Reasoner, M.A., 1992. Evaluation of differential pollen deposition and pollen focussing from three Holocene intervals in sediments from Lake O'Hara, Yoho National Park, British Columbia, Canada: intra-lake variability in pollen percentages, concentrations and influx. Review of Palaeobotany and Palynology 75, (1-2), 103-131.

Beck, C., Reyss, J.-L., Leclerc, F., Moreno, E., Feuillet, N., Barrier, L., et al. (2012). Identification of deep subaqueous co-seismic scarps through specific coeval sedimentation in Lesser Antilles: implication for seismic hazard. Natural Hazards and Earth System Sciences 12(5), 1755–1767.

Beug, H.-J., 2004. Leitfaden der Pollenbestimmung für Mitteleuropa und angrenzende Gebiete, Pfeil, Munich.

Birks, H.J.B., Birks, H.H., 1980. Quaternary Palaeoecology, Edward Arnold, London.

576 Blaauw, M., 2010. Methods and code for 'classical' age-modelling of radiocarbon sequences.
577 Quaternary Geochronology 5, 512–518. https://doi.org/10.1016/j.quageo.2010.01.002
578
579 Blaauw, M., Christen, J.A., 2011. Flexible paleoclimate age-depth models using an autoregressive
580 gamma process. Bayesian Analysis. 6:3. pp 457-474.
581
582 Bohn, U., Gollub, G., Hettwer, C., 2000. Karte der natürlichen Vegetation Europas, Bundesamt für
583 Naturschutz Federal Agency for Nature Conservation, Bohn-Bad Godesberg.
584
585 Bottema, S., 1986. A late Quaternary pollen diagram from Lake Urmia (northwestern Iran). Review of
586 Palaeobotany and Palynology 47, 241-261.
587
588 Çağatay, M.N., Öğretmen, N., Damcı, E., Stockhecke, M., Sancar, Ü., Eriş, K.K., Özeren, S., 2014. Lake
589 level and climate records of the last 90ka from the Northern Basin of Lake Van, eastern Turkey,
590 Quaternary Science Reviews 104, 97-116.
591 Chapron, E., Simonneau, A., Ledoux, G., Arnaud, F., Lajeunesse, P., Albéric, P., 2016. French Alpine
592 Foreland Holocene Paleoseismicity Revealed by Coeval Mass Wasting Deposits inGlacial Lakes.
593 Submarine Mass Movements and their Consequences, V, 341-349.
594
595 Cohen, A.S., 2003. Paleolimnology. The history and evolution of lake systems. Oxford University
596 Press, New York
597
598 Connor, S., Colombaroli, D., Confortini, F., Gobet, E., Ilyashuk, B.P., Ilyashuk, E.A., van Leeuwen,
599 J.F.N., Lamentowicz, M., O van der Knaap, W., Malysheva, E., Marchetto, A., Margalitadze, N. Mazei,
600 Y., Mitchell, E.A.D., Payne, R.J., Ammann, B., 2018. Long term population dynamics - theory and
601 reality in a peatland ecosystem. Journal of Ecology, 1-51.
602
603 Connor, S. E., Sagona, A., 2007. Environment and society in the late prehistory of Southern Georgia,
604 Caucasus. In: Lyonnet, B., (Ed.) Les cultures du Caucase (VIe-IIIe millénaires avant notre ère) – Leurs
605 relations avec le Proche-Orient. Editions Recherche sur les Civilisations. Paris CNRS Editions. pp. 21-
606 36.
607
608 Connor, S.E., 2011. A Promethean Legacy: Late Quaternary Vegetation History of Southern Georgia,
609 the Caucasus. Peeters, Louvain
610

611 Connor, S.E., Kvavadze, E.V., 2008. Modelling late Quaternary changes in plant distribution,
612 vegetation and climate using pollen data from Georgia, Caucasus. Journal of Biogeography 36 (3),
613 529-545.
614
615 Connor, S.E., Ross, S.A., Sobotkova, A., Herries, A.I.R., Mooney, S.D., Longford, C., Iliev, I., 2013.
616 Environmental conditions in the SE Balkans sine the Last Glacial Maximum and their influence on the
617 spread of agriculture into Europe. Quaternary Science Reviews 68, 200–215.
618
619 Connor, S.E., Thomas, I., Kvavadze, E., Arabuli, G.J., Avakov, G., Sagona, A., 2004. A survey modern
620 pollen and vegetation along an altitudinal transect in southern Georgia, Caucasus region. Review of
621 Palaeobotany and Palynology 129, 229-250.
622
623 de Klerk, P., Haberl, A., Kaffke, A., Krebs, M., Matchutadze, I., Minke, M., Schulz, J., Joosten, H., 2009.
624 Vegetation history and environmental development since ca 6000 cal yr BP in and around Ispani 2
625 (Kolkheti lowlands, Georgia). Quaternary Science Reviews 28, 890-910.
626
627 Dean, J.R., Jones, M.D., Leng, M.J., Noble, S.R., Metcalfe, S.E., Sloane, H.J., Sahy, D., Eastwood, W.J.,
628 Roberts, C.N. 2015. Eastern Mediterranean hydroclimate over the late glacial and Holocene,
629 reconstructed from the sediments of Nar lake, central Turkey, using stable isotopes and carbonate
630 mineralogy, Quaternary Science Reviews, 124, 162-174
631
632 Djamali, M., Akhani, H., Andrieu-Ponel, V., Braconnot, P., Brewer, S., de Beaulieu, J.-L., Fleitmann, D.,
633 Fleury, J., Gasse, F., Guibal, F., Jackson, S.T., Lézine, A.-M., Médail, F., Ponel, P., Roberts, N., Stevens,
634 L.R., 2010. Indian summer monsoon variations could have affected the early-Holocene woodland
635 expansion in the Near East. The Holocene 20, 813-820.
636
637 Djamali, M., de Beaulieu, J.-L., Shah-hosseini, M., Andrieu-Ponel, V., Ponel, P., Amini, A., Akhani, H.,
638 Leroy, S.A.G., Stevens, L., Lahijani, H., Brewer, S., 2008. A late Pleistocene long pollen record from
639 Lake Urmia, NW Iran. Quaternary Research 69 (3), 413-420
640
641 Fægri, K., Iversen, J., 1989. Textbook of pollen analysis (revised by Fægri, K., Kaland, P.E. and
642 Krzywinski, K.). John Wiley and Sons.
643
644 Fox, J., 2016. Using the R Commander: A Point-and-Click Interface for R, 1st ed. Chapman and
645 Hall/CRC. https://doi.org/10.1201/9781315380537

Girard, M., Renault-Miskovsky, J., 1969. Nouvelles techniques de préparations en palynologie, appliquées à trois sédiments du Quaternaire final de l'Abri Cornille (Istres, Bouches-du-Rhone). Bulletin de l'AFEQ 21 (4), 275-284.

Goeury, C., Beaulieu, J.L. de, 1979. A propos de la concentration du pollen à l'aide de la liqueur de Thoulet dans les sédiments minéraux. Pollen Spores 21, 239-251.

Grimm, E., 1987. CONISS: a Fortran 77 Program for stratigraphically constraint cluster analysis by the method of incremental squares. Computers and Geosciences 13, 13-35.

Hamon, C., Jalabadze, M., Agapishvili, T., Baudouin, E., Koridze, I., Messager, E., 2016. Gadachrili Gora: Architecture and organisation of a Neolithic settlement in the middle Kura Valley (6th millennium BC, Georgia). Quaternary International 395, 154-169

Heiri, O., Lotter, A.F., Lemcke, G. 2001. Loss on ignition as a method for estimating organic and carbonate content in sediments: reproducibility and comparability of results. Journal of Paleolimnology 25, 101-110.

Huntley, B., Birks, H.J.B., 1983. An Atlas of Past and Present Pollen Maps for Europe: 0-13000 years ago. Cambridge University Press, Cambridge.

Huttunen, P., Stober, J. 1980. Dating of palaeomagnetic records from Finnish lake sediment cores using pollen analysis. Boreas, 9 (3), 193-202

Joannin, S., Ali, A. A., Ollivier, V., Roiron, P., Peyron, O., Chevaux, S., Nahapetyan, S., Tozalakyan, P., Karakhanyan, A., Chataigner, C., 2014. Vegetation, fire and climate history of the Lesser Caucasus: a new Holocene record from Zarishat fen (Armenia), Journal of Quaternary Science 29, 70-82.

Jones, M.D., Roberts, C.N., Leng, M.J., 2007. Quantifying climatic change through the last glacial–interglacial transition based on lake isotope palaeohydrology from central Turkey. Quaternary Research 67, 463-473.

Kachakhidze, M., Kachakhidze, N., Kiladze, R., Kukhianidze, V., Ramishvili, G. 2003. Relatively small earth-quakes of Javakheti Highland as the precursors of large earthquakes occurring in the Caucasus.

Natural Hazards and Earth System Science, Copernicus Publications on behalf of the European GeosciencesUnion, 2003, 3 (3/4), pp.165-170. hal-00299012

Kadowaki S., Maher, L. Portillo, M., Albert, R.M. Akashi, C., Guliyev, F., Nishiaki, Y., 2015. Geoarchaeological and palaeobotanical evidence for prehistoric cereal storage in the southern Caucasus: the Neolithic settlement of Göytepe (mid 8th millennium BP), Journal of Archaeological Science 53, 408-425.

Kakhiani, K., Sagona, A., Sagona, C., Kvavadze, E., Bedianashvili, G., Messager, E., Martin, L., Herrscher, E., Martkoplishvili, I., Birkett-Rees, J., Longford, C., 2013. Archaeological Investigations at Chobareti in southern Georgia, the Caucasus. Ancient Near Eastern Studies 50, 1-138.

Koning, E., Epping, E., and Van Raaphorst, W., 2002. Determining Biogenic Silica in Marine Samples by Tracking Silicate and Aluminium Concentrations in Alkaline Leaching Solutions. Aquatic Geochemistry 8, 37–67.

Kuzucuoğlu, C., Christol, L., Mouralis, D., Doğu, A.F., Akköprü, E., Fort, M., Brunsteın, D., Zorer, H., Fontugne, M., Karabıyıkoğlu, M., 2010. Formation of the Upper Pleistocene terraces of Lake Van (Turkey). Journal of Quaternary Sciences 25, 1124-1137.

Kvavadze E.V., 1993. On the interpretation of subfossil spore-pollen spectra in the mountains. Acta Palaeobotanica 33, 347-360.

Kvavadze E.V., Connor, S.E., 2005. Zelkova carpinifolia (Pallas) K. Koch in Holocene sediments of Georgia - an indicator of climatic optima, Review of Palaeobotany and Palynology 133, 69-89.

Kvavadze, E.V., Kakhiani, K., 2010. Palynology of the Paravani burial mound (Early Bronze Age, Georgia). Vegetation History and Archaeobotany 19 (5-6), 469-478.

Lê, S., Josse, J., Husson, F., 2008. FactoMineR: An R Package for Multivariate Analysis. J. Stat. Soft. 25. https://doi.org/10.18637/jss.v025.i01

Lebedev, V.A., Bubnov, S.N., Dudauri, O.Z., Vashakidze, G.T., 2008. Geochronology of Pliocene Volcanism in the Dzhavakheti Highland (the Lesser Caucasus). Part 2: Eastern Part of the Dzhavakheti Highland. Regional Geological Correlation Stratigraphy and Geological Correlation 16, 553-574.

716

717 Lemcke, G., Sturm, M., 1997. δ18o and Trace Element Measurements as Proxy for the Reconstruction
718 of Climate Changes at Lake Van (Turkey): Preliminary Results. In: Dalfes, H.N., Kukla, G., Weiss, H.
719 (Eds.), Third Millennium BC Climate Change and old World Collapse, NATO ASI Series. Springer, Berlin
720 Heidelberg, pp. 653-678.

721

722 Leroy, S.A.G., Arpe, K., 2007. Glacial refugia for summer-green trees in Europe and S-W Asia as
723 proposed by ECHAM3 time-slice atmospheric model simulations. Journal of Biogeography 34, 2115-
724 2128.

725

726 Leroy, S.A.G., Lopez-Merino, L., Tudryn, A., Chalie, F., Gasse, F., 2014. Late Pleistocene and Holocene
727 palaeoenvironments in and around the middle Caspian basin as reconstructed from a deep-sea core.
728 Quaternary Science Reviews 101, 91–110.

729

730 Leroy, S.A.G., Tudryn, A., Chalie, F., Lopez-Merino, L., Gasse, F., 2013. From the Allerød to the mid-
731 Holocene: palynological evidence from the south basin of the Caspian Sea. Quaternary Science
732 Reviews 78, 77–97.

733

734 Leroyer, C., Joannin, S., Aoustin, D., Ali, A.A., Peyron, O., Ollivier, V., Tozalakyan, P., Karakhanyan, A.,
735 Jude, F., 2016. Mid Holocene vegetation reconstruction from Vanevan peat (south-eastern shore of
736 Lake Sevan, Armenia), Quaternary International 395, 5-18.

737

738 Litt, T., Krastel, S., Sturm, M., Kipfer, R., Örcen, S., Heumann, G., Franz, S.O., Ülgen, U. B., Niessen, F.,
739 'PALEOVAN', International Continental Scientific Drilling Program (ICDP): site survey results and
740 perspectives. Quaternary Science Reviews 28 (15-16), 1555-1567.

741

742 Litt, T., Pickarski, N., Heumann, G., Stockhecke, M., Tzedakis, P.C., 2014. A 600,000 years long
743 continental pollen record from Lake Van, eastern Anatolia (Turkey). Quaternary Science Reviews 104,
744 30–41.

745

746 Lyonnet, B., Guliyev, F., Bouquet, L. Bruley-Chabot, G., Samzun, A., Pecqueur, L., Jovenet, E.,
747 Baudouin, E., Fontugne, M. Raymond, P., Degorre, E., Astruc, L., Guilbeau, D., Le Dosseur, G.,
748 Benecke, N., Hamon, C., Poulmarc'h, M., Courcier, A., 2016. Mentesh Tepe, an early settlement of
749 the Shomu-Shulaveri Culture in Azerbaijan, Quaternary International 395, 170-183.

750

751 Matcharashvili, I., Arabuli, G., Darchiashvili, G., Gorgadze, G., 2004. Javakheti Wetlands: Biodiversity
752 and Conservation [In Georgian and English]. NACRES, Tbilisi, Georgia.
753
754 Margalitadze, N.A., 1995. Istoriia golotsenovoi rastitel'nosti Gruzii. Metsniereba, Tbilisi (in Russian).
755 Matcharashvili, I., Arabuli, G., Darchiashvili, G., Gorgadze, G., 2004. Javakheti Wetlands: Biodiversity
756 and Conservation. NACRES, Tbilisi.
757
758 Messager, E., Belmecheri, S., von Grafenstein, U., Nomade, S., Ollivier, V., Voinchet, P., Puaud, S.,
759 Courtin-Nomade, A., Guillou, H., Mgeladze, A., Dumoulin, J.P., Mazuy, A., Lordkipanidze, D., 2013.
760 Late Quaternary record of the vegetation and catchment-related changes from Lake Paravani
761 (Javakheti, South Caucasus). Quaternary Science Reviews 77, 125-140.
762
763 Messager, E., Nomade, S., Wilhelm, B., Joannin, S., Scao, V., von Grafenstein, U., Martkoplishvili, I.,
764 Ollivier, V., Mgeladze, A., Dumoulin, J.P., Mazuy, A., Belmecheri, S., Lordkipanidze, D., 2017. New
765 pollen evidence for a delay in post−glacial forest expansion in the South Caucasus, the Nariani record.
766 Quaternary Research 87, 121-132.
767
768 Nakhutsrishvili, G.S., 1999. The vegetation of Georgia (Caucasus). Braun-Blanquetia 15, 1-68.
769
770 Nomade, S., Scao, V., Guillou, H., Messager, E., Mgeladze, A., Voinchet, P., Renne, P.R., Courtin-
771 Nomade, A., Bardintzeff, J.M., Ferring, R., Lordkipanidze, D., 2016. New 40Ar/39Ar, unspiked K/Ar
772 and geochemical constraints on the Pleistocene magmatism of the Samtskhe-Javakheti highlands
773 (Republic of Georgia), Quaternary International 395, 45-59.
774
775 North Greenland Ice Core Project Members, 2004. North Greenland Ice Core Project Members High-
776 resolution record of Northern Hemisphere climate extending into the Last Interglacial period. Nature
777 431, 147-151.
778
779 Nutz, A., Schuster, M., Ghienne, JF. et al., 2018. Wind-driven waterbodies: a new category of lake
780 within an alternative sedimentologically-based lake classification. Journal of Paleolimnology 59 (2),
781 189–199.
782
783 Pickarski, N., Kwiecien, O., Djamali, M., Litt, T., 2015. Vegetation and environmental changes during
784 the last interglacial in eastern Anatolia (Turkey): a new high-resolution pollen record from Lake Van:
785 palaeogeography, Palaeoclimatology, Palaeoecology 435, 145-158.

Philip, H., Avagyan, A.V., Karakhanian, A.S., Ritz, J.-F., Rebai, S. 2001. Slip rates and recurrence intervals of strong earthquakes along the Pambak-Sevan-Sunik fault (Armenia). Tectonophysics 343, 205-232.

R Core Team, 2018. R: A language and environment for statistical computing. R Foundation for Statistical Computing. Vienna, Austria.

Ragueneau, O., Savoye, N., Del Amo, Y., Cotten, J., Tardiveau, B., Leynaert, A., 2005. A New Method for the Measurement of Biogenic Silica in Suspended Matter of Coastal Waters: Using Si:Al Ratios to Correct for the Mineral Interference. Continental Shelf Research 25, 697-710.

Ritz, J.-F., Avagyan, A., Mkrtchyan, M., Nazari, H., Blard, P.-H., Karakhanian, A., Philip, H., Balescu, S., Mahan, S., Huot, S., Munch, P., Lamothe, M., 2016. Active tectonics within the NW and SE extensions of the Pampak-Sevan-Syunik fault: Implications for the present geodynamics of Armenia, Quaternary International 395, 61-78.

Reille, M., 1992. Pollen et Spores d'Europe et d'Afrique du Nord. Laboratoire de Botanique Historique et Palynologie. U.R.A. C.N.R.S. 1152, Marseille.

Reimer, P.J., Bard, E., Bayliss, A., Beck, J. W., Blackwell, P. G., Bronk Ramsey, C., Buck, C. E., Cheng, H., Edwards, R. L., Friedrich, M., Grootes, P. M., Guilderson, T. P., Haflidason, H., Hajdas, I., Hatt, C., Heaton, T.J., Hogg, A.G., Hughen, K.A., Kaiser, K.F., Kromer, B., Manning, S.W., Niu, M., Reimer, R.W., Richards, D.A., Scott, E.M., Southon, J.R., Turney, C.S.M., van der Plicht, J., 2013. IntCal13 and MARINE13 radiocarbon age calibration curves 0–50000 years cal BP, Radiocarbon 55, 1869-1887.

Roberts, N., 2002. Did prehistoric landscape management retard the post-glacial spread of woodland in Southwest Asia? Antiquity 76, 1002-1010.

Roberts, N., Reed, J.M., Leng, M.J., Kuzucuoğlu, C., Fontugne, M., Bertaux, J., Woldring, H., Bottema, S., Black, S., Hunt, E., Karabıyıkoğlu, M., 2001. The tempo of Holocene climatic change in the eastern Mediterranean region: new high-resolution craterlake sediment data from central Turkey. The Holocene 11, 721-736.

820 Rossignol-Strick, M., 1995. Sea-land correlation of pollen records in the eastern Mediterranean for
821 the glacial-interglacial transition: biostratigraphy versus radiometric time-scale. Quaternary Science
822 Reviews 14, 293-315.
823
824 Ryabogina, N., Borisov, A., Idrisov, I., Bakushev, M., 2019. Holocene environmental history and
825 populating of mountainous Dagestan (Eastern Caucasus, Russia). Quaternary International 516, 111-
826 126.
827
828 Sabatier, P., Dezileau, L., Briqueu, L., Colin, C., Siani, G., 2010. Clay minerals and geochemistry
829 record from northwest Mediterranean coastal lagoon sequence: implications for paleostorm
830 reconstruction. Sediment. Geol. 228, 205–217.
831
832 Shumilovskikh, L., Tarasov, P., Arz, H.W., Fleitmann, D., Marret, F., Nowaczyk, N., Plessen, B., Schlütz,
833 F., Behling, H., 2012. Vegetation and environmental dynamics in the southern Black Sea region since
834 18 kyr BP derived from the marine core 22-GC3. Palaeogeography, Palaeoclimatology, Palaeoecology
835 337-338, 177-193.
836
837 Stevens, L.R., Ito, E., Schwalb, A., Wright, H.E., 2006. Timing of atmospheric precipitation in the
838 Zagros Mountains inferred from a multi-proxy record from Lake Mirabad, Iran. Quaternary Research
839 66, 494-500.
840 Stevens, L.R., Wright, H.E., Ito, E., 2001. Proposed changes in seasonality of climate during the
841 Lateglacial and Holocene at Lake Zeribar, Iran. The Holocene 11, 747-755.
842
843 Turner, R., Roberts N., Eastwood W.J., Jenkins, E., Rosen, A., 2010. Fire, climate and the origins of
844 agriculture: micro-charcoal records of biomass burning during the last glacial-interglacial transition in
845 Southwest Asia. Journal of Quaternary Science 25, 371-386.
846
847 Van Zeist, W., Bottema, S., 1977. Palynological investigations in western Iran. Palaeohistoria 24, 19-
848 85.
849 van Zeist, W., Bottema, S., 1991. Late Quaternary vegetation of the Near East. Beihefte zum Tubinger
850 Atlas des Vorderen Orients, Reihe A18, Wiesbadeni: Dr L. Reichert Verlag, 156 pp.
851
852 Varoutsikos, B. Mgeladze A., Chahoud, J., Gabunia, M., Agapishvili, T., Martin, L., Chataigner, C.,
853 2017. From the Mesolithic to the Chalcolithic in the South Caucasus: New data from the Bavra Ablari
854 rock shelter. In: Batmaz A., Bedianashvili G., Michalewicz A.,Robinson A. Context and Connection:

855 Essays on the Archaeology of the Ancient Near East in Honour of Antonio Sagona. Leuven: Peeters,
856 2017.
857
858 Wick, L., Lemcke, G. Sturm, M., 2003. Evidence of Lateglacial and Holocene climatic change and
859 human impact in eastern Anatolia: high resolution pollen, charcoal, isotopic and geochemical records
860 from the laminated sediments of Lake Van, Turkey. The Holocene 13, 665-675.
861
862 Wilhelm, B., Vogel, H., Crouzet C., Etienne, D. and Anselmetti, F.S. 2016a. Frequency and intensity of
863 palaeofloods at the interface of Atlantic and Mediterranean climate domains. Climate of the Past, 12,
864 299-316
865
866 Wilhelm, B., Nomade, J., Crouzet, C., Litty, C., Sabatier, P., Belle, S., Rolland, Y., Revel, M.,
867 Courboulex, F., Arnaud, F., Anselmetti, F.S. 2016b. Quantified sensitivity of lake sediments to record
868 historic earthquakes: Implications for paleoseismology. Journal of Geophysical Research, 121(1), 2–
869 16.
870
871 Wright, H.E., Jr, Ammann, B., Stefanova, I., Atanassova, J., Margalitadze, N., Wick, L., Blyakharchuk,
872 T., 2003. Lateglacial and Early-Holocene dry climates from the Balkan peninsula to southern Siberia.
873 Aspects of palynology and palaeoecology (ed. by S. Tonkov), Pensoft, Sofia-Moscow, pp. 127-136.
874

Figure captions

Figure 1: Geological map of the Javakheti Plateau, locations of cores PAR09-01 and PAR12-04 in Lake Paravani (modified from Nomade et al., 2016).

Figure 2. Vegetation map of the region, (prepared using EuroVegMap software, Bohn et al., 2000).

Figure 3. Lithology, LOI analysis, magnetic susceptibility and XRF data for cores PAR09-01 and PAR12-04. Radiocarbon ages and locations are indicated along the stratigraphy.

Figure 4. Principal component analysis (PCA) performed on major elements (Al, Si, K, Ti, Ca and Fe intensities) measured by XRF core scanner. The samples have been coloured by unit.

Figure 5. Age-depth Model of PAR12-04 and PAR09-01

Figure 6. Synthetic pollen diagram (+ CONISS analysis) of the PAR12-04 core

Figure 7. Puzzle made of Paravani lake sediment units

Figure 8. Correlations of the PAR12-04 and PAR09-01 sequences.

Table captions

Table 1. List of AMS ^{14}C dates from cores PAR09-01 and PAR12-04.

Table 2. Description of PAR 12-04 and PAR 09-01 units

Supplementary data captions

Supplementary Figure 1. Physiographic map of the region, showing Paravani (yellow star) and pollen records discussed in the text (white stars). (The map is adapted from GeoAtlas).

Supplementary Figure 2. XRF core scanner curves of two elements (K and Ti) and the ratio Si/Al for six sequences collected in the Lake Paravani

Supplementary Figure 3. Si/Al ratio along the PAR12-04 core, and photos of microscopic slides of bulk sediment prepared for each unit (red circles correspond to diatoms)

Supplementary Figure 4. Si/Al, Ti/Al and Fe/Al ratios along the PAR12-04 and PAR09-01 cores

Supplementary Figure 5. Synthetic pollen diagram of PAR 12-04 and PAR 09-01 cores

Supplementary Figure 6. Comparison of regional pollen records (Arboreal Pollen, Poaceae and steppic plants): Zarishat (Joannin et al., 2014), Van (Litt et al., 2012; Pickarski et al., 2015), Nariani (Messager et al., 2017), Paravani (this study) and Dedichara (Connor et al., 2018). The Paravani synthetic curves are composed of PAR12-04 pollen data (lower part) and PAR09-01 pollen data (upper part). The Dedichara pollen data are from the European Pollen Database, available in the Neotoma Paleoecology Database.

Figure 1

Click here to access/download;Figure;Fig 1 Geology Paravani 29 10.tif

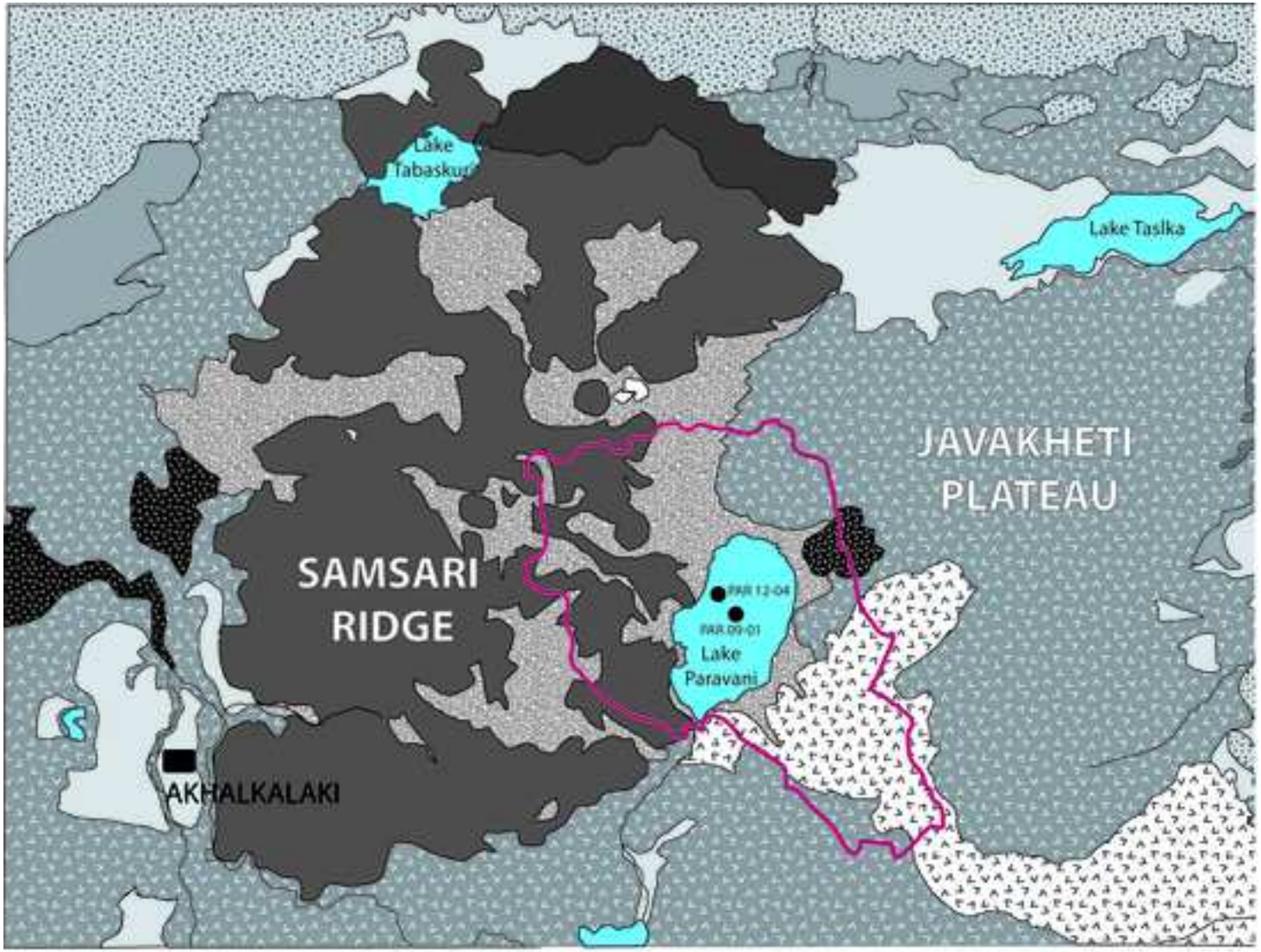

Figure 2

Click here to access/download;Figure;Fig 2 vegetation map 29 10.tif

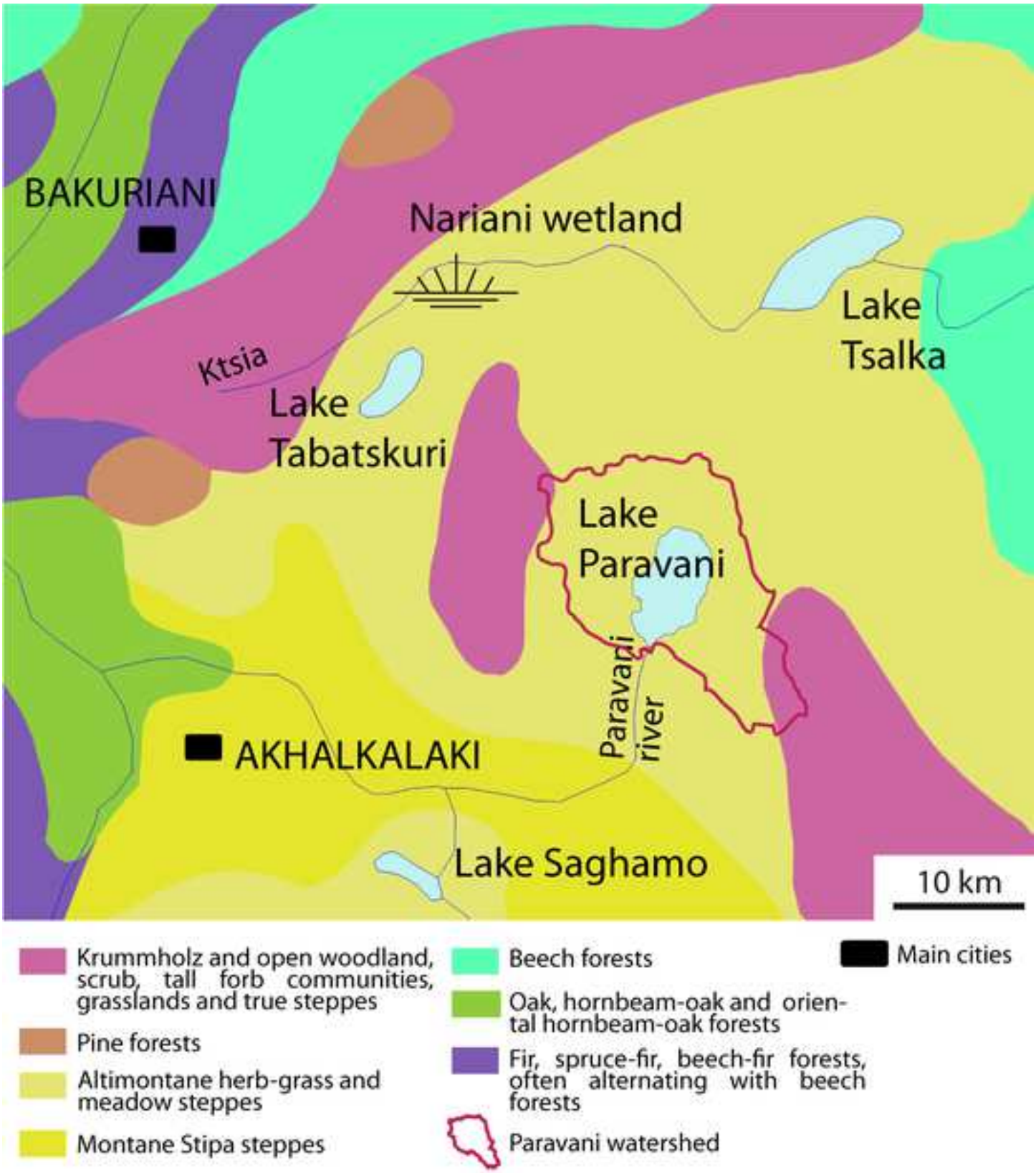

Figure 3

Click here to access/download;Figure;Fig 3 log loi sm xrf age 29 10.tif

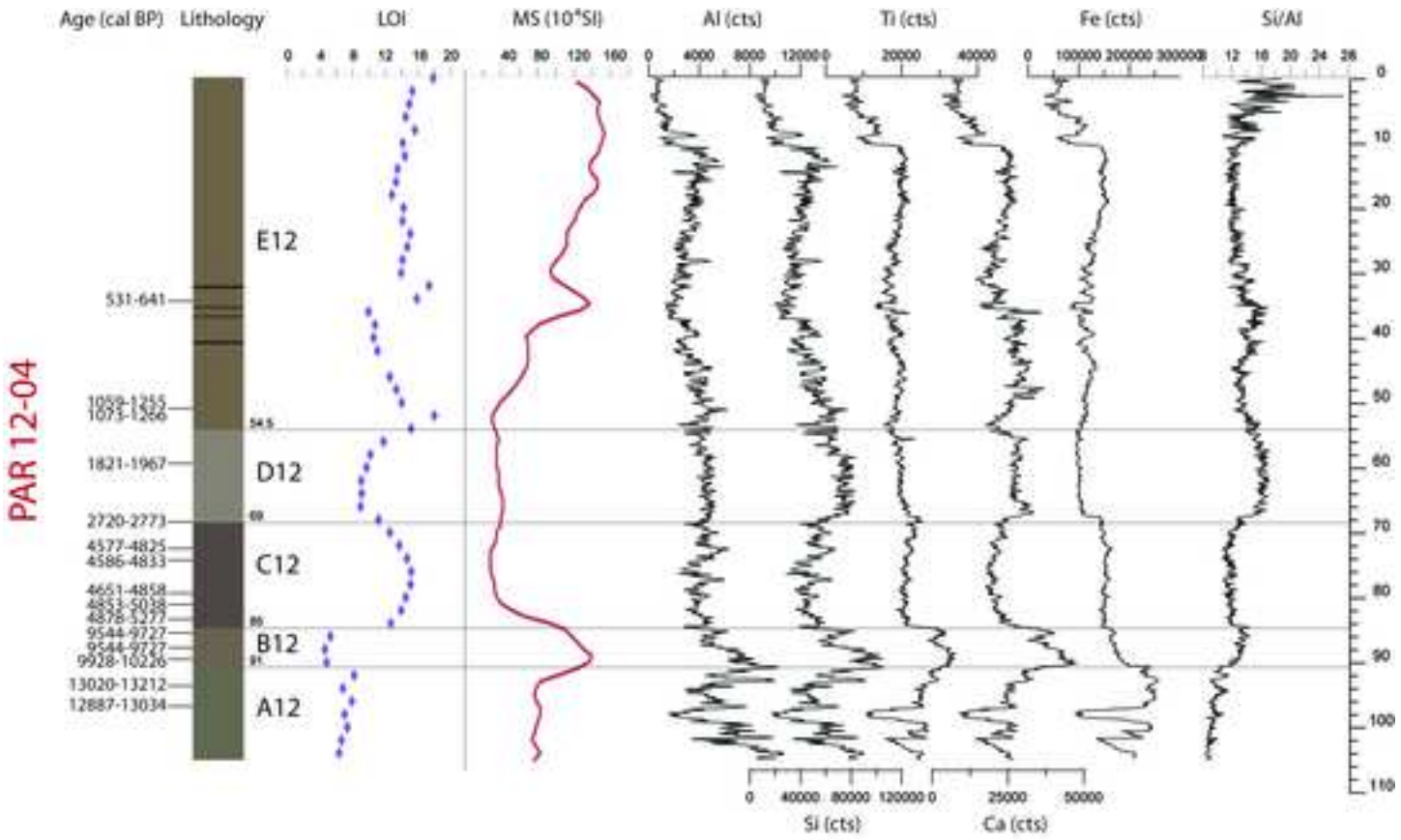

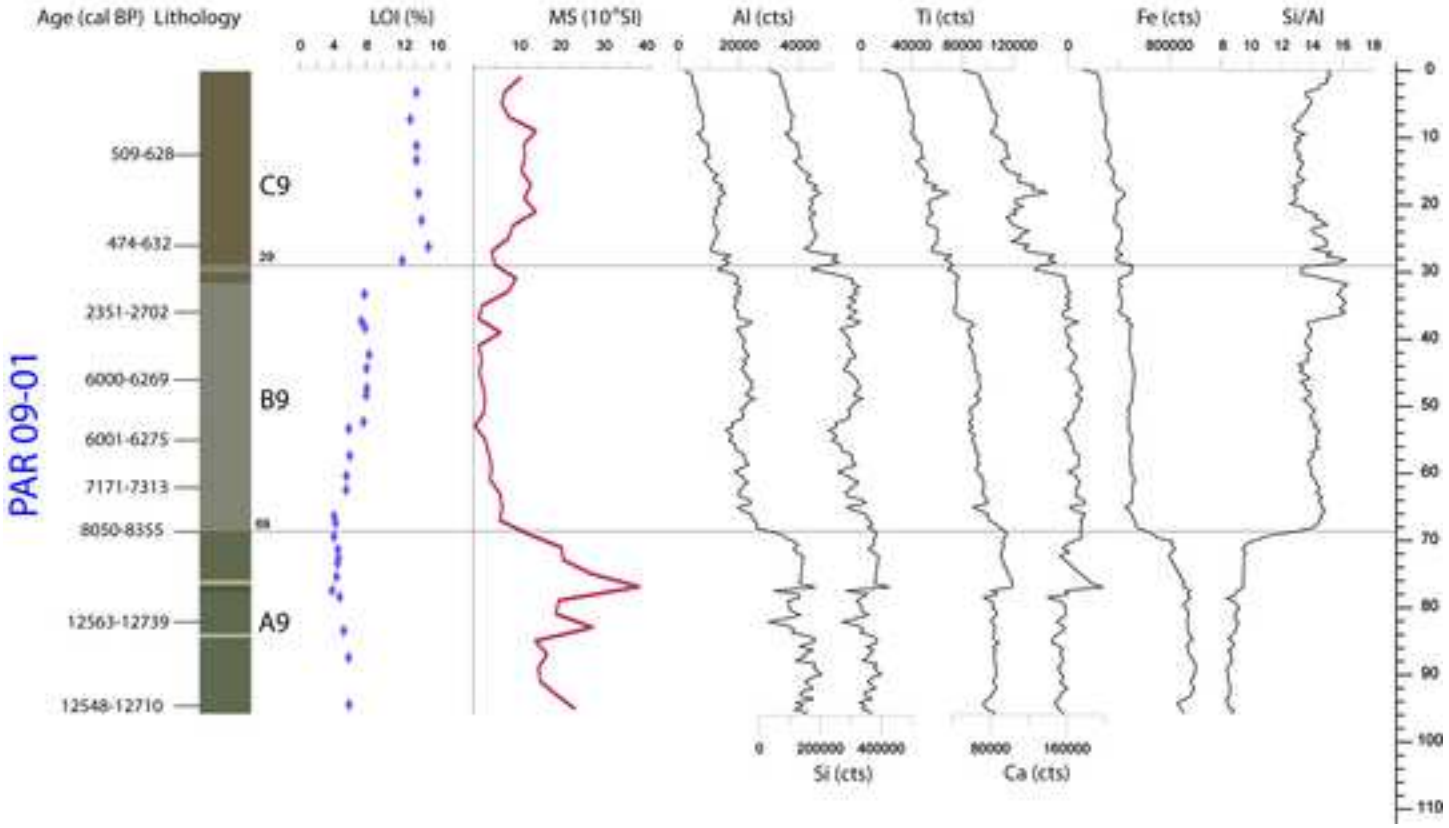

Figure 4

Click here to access/download;Figure;Fig 4 ACP XRF 29 10.tif

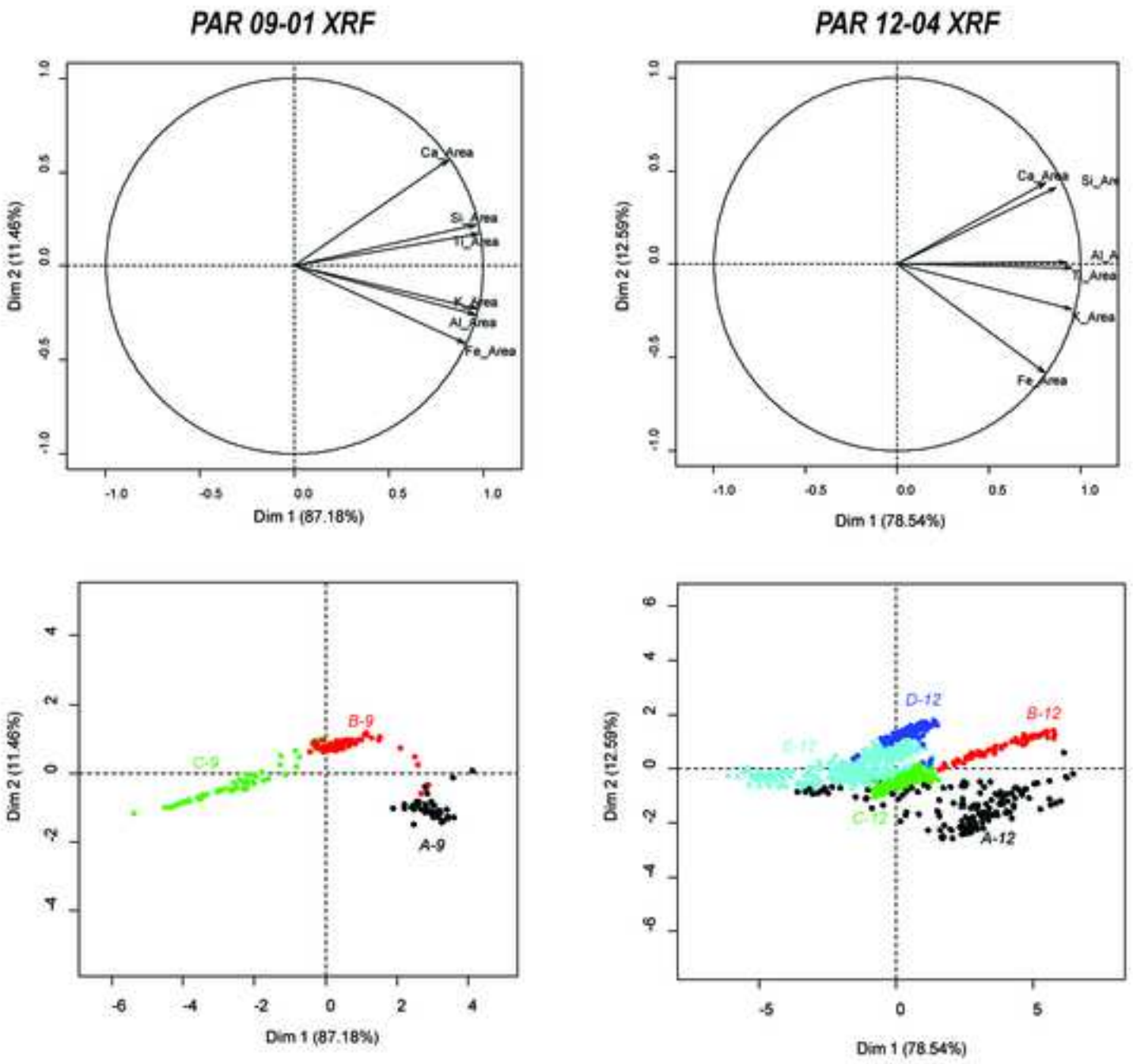

Figure 5

Click here to access/download;Figure;Fig 5 Age depth model 29 10.tif

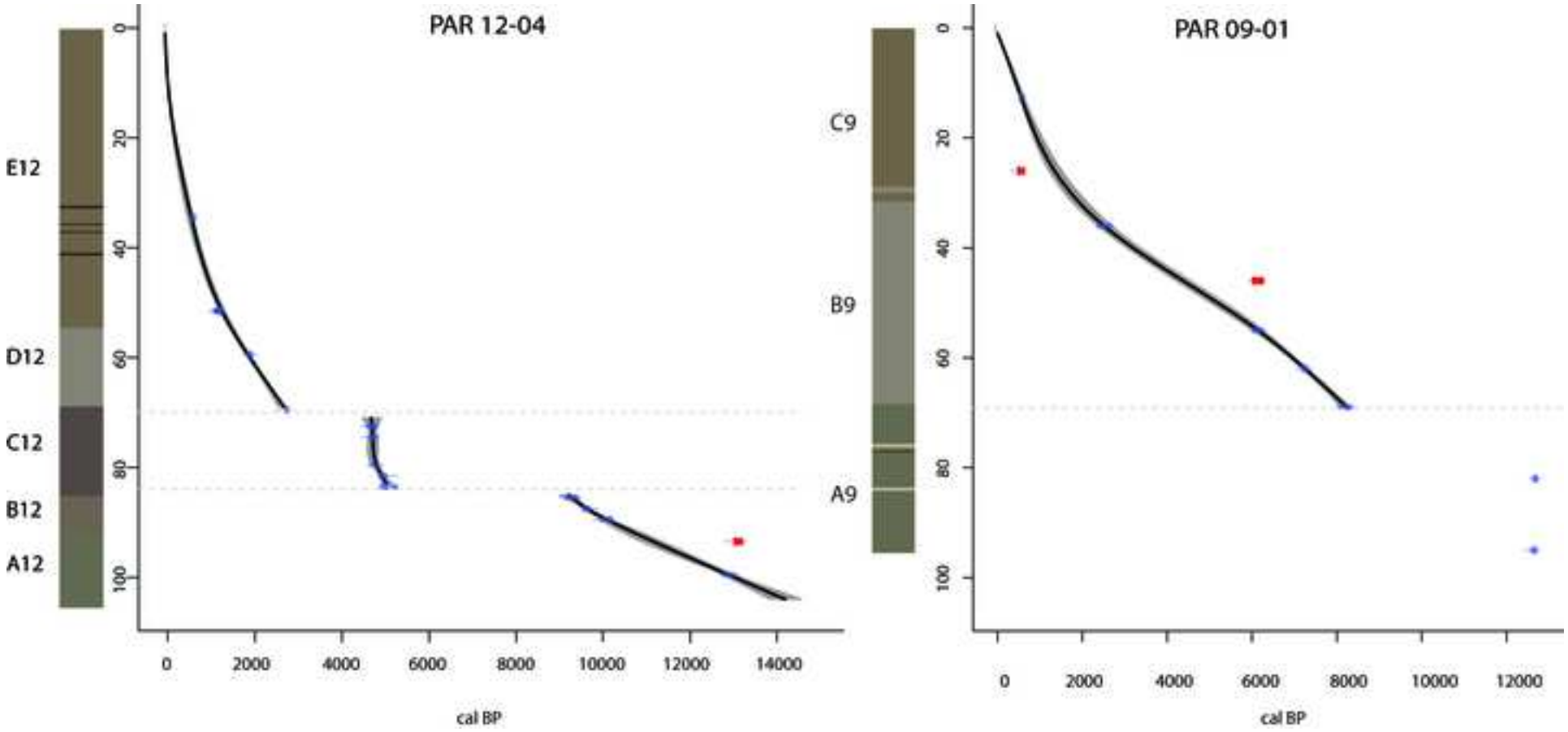

Figure 6

Click here to access/download;Figure;Fig 6 pollen par1204 29 10.tif

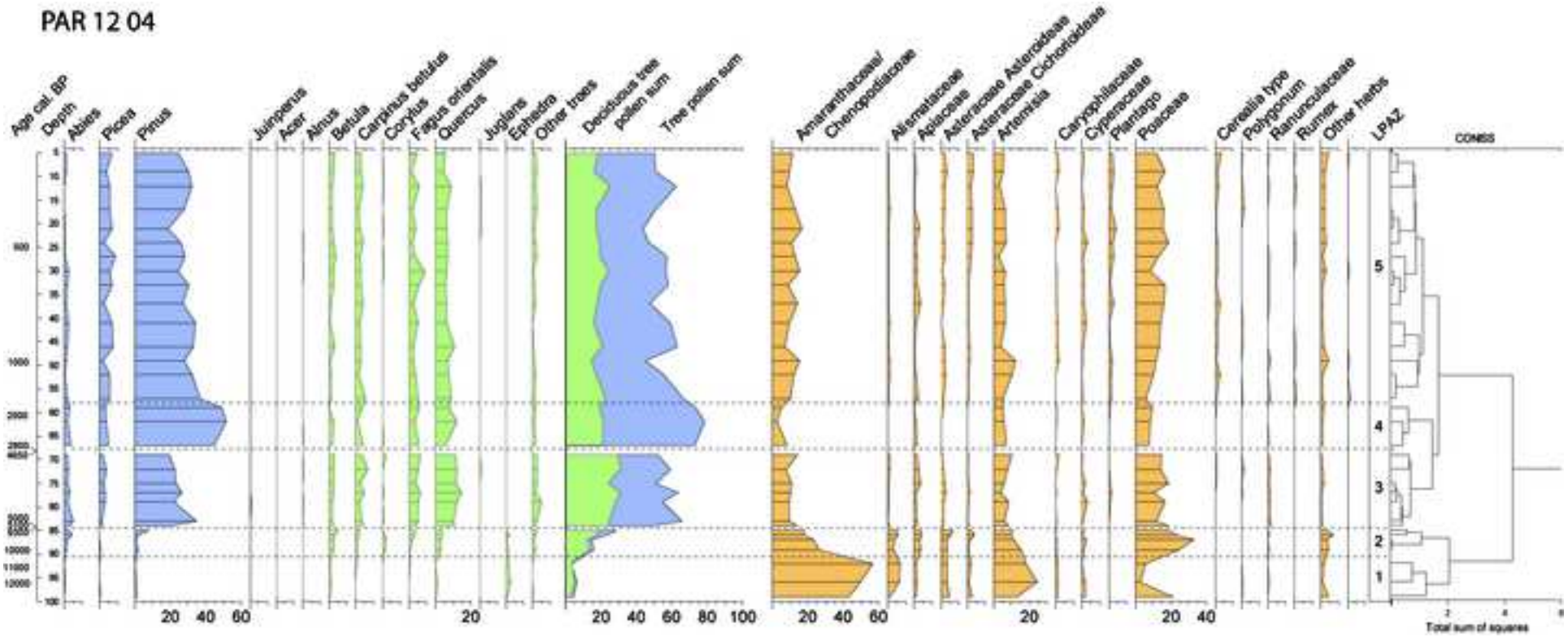

Figure 7

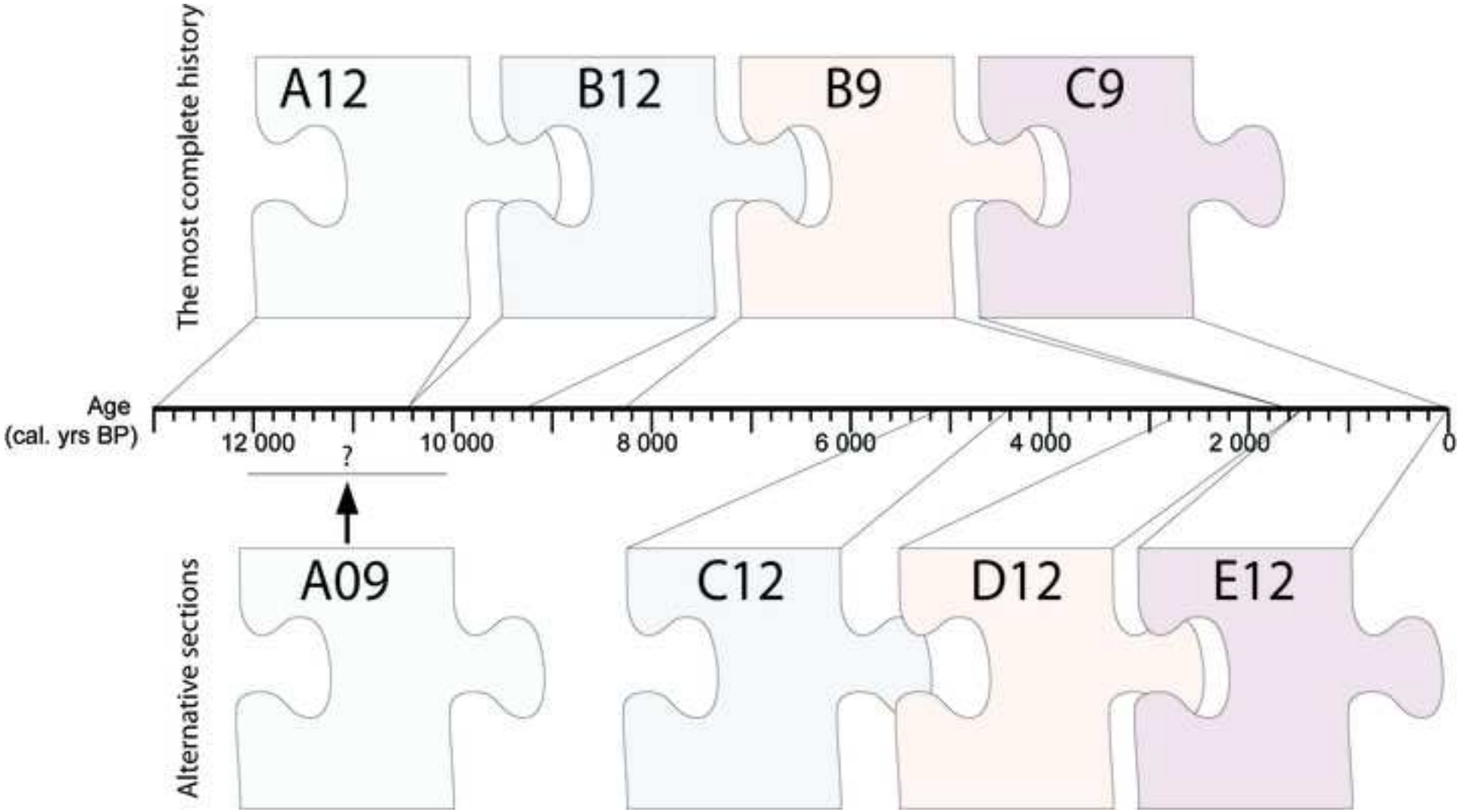

Figure 8

Click here to access/download;Figure;fig 8 synthese 29 10.tif

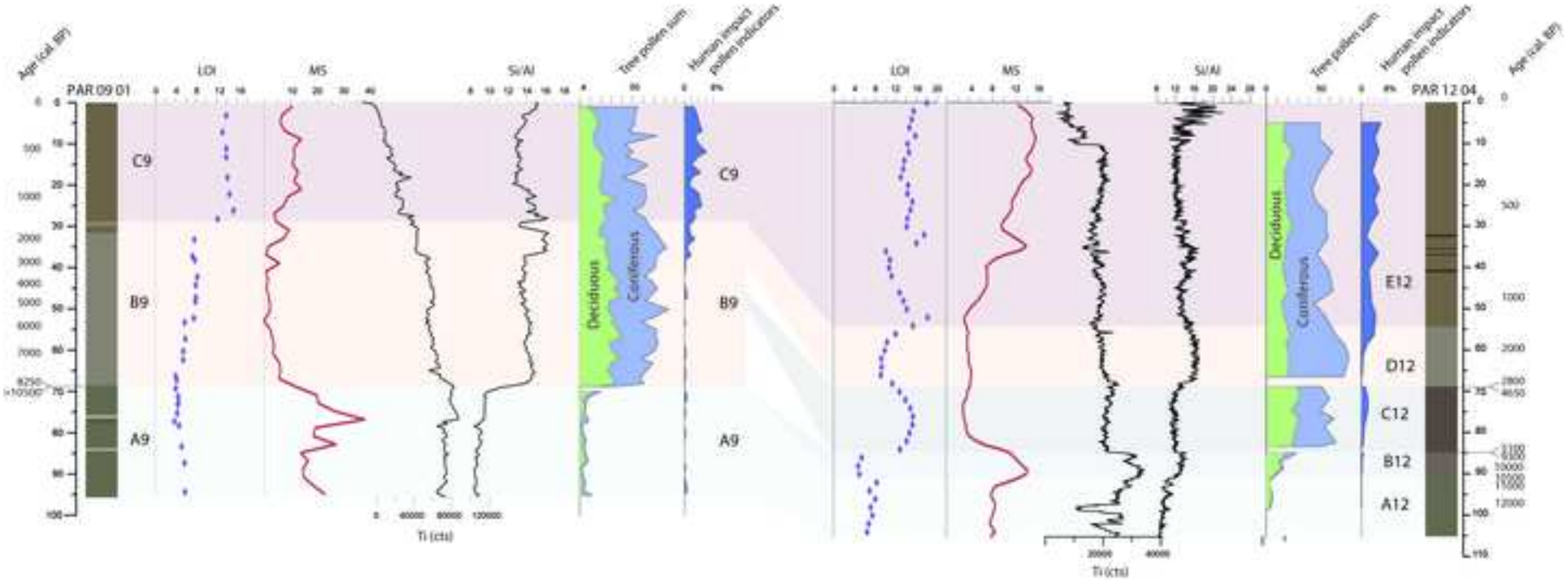

Table 1

Click here to access/download

Table

Table 1.xlsx

Table 2

Click here to access/download

Table

Table 2.xlsx